This is a repository copy of *Improved Temperature Performance of 1.31-mu/m Quantum Dot Lasers by Optimized Ridge Waveguide Design* .

White Rose Research Online URL for this paper:
http://eprints.whiterose.ac.uk/816/

Article:

Ray, S.K., Groom, K.M., Hogg, R.A. et al. (5 more authors) (2005) Improved Temperature Performance of 1.31-mu/m Quantum Dot Lasers by Optimized Ridge Waveguide Design. IEEE Photonics Technology Letters, 17 (9). pp. 1785-1787. ISSN 1041-1135

https://doi.org/10.1109/LPT.2005.853530

Reuse

Unless indicated otherwise, fulltext items are protected by copyright with all rights reserved. The copyright exception in section 29 of the Copyright, Designs and Patents Act 1988 allows the making of a single copy solely for the purpose of non-commercial research or private study within the limits of fair dealing. The publisher or other rights-holder may allow further reproduction and re-use of this version - refer to the White Rose Research Online record for this item. Where records identify the publisher as the copyright holder, users can verify any specific terms of use on the publisher's website.

Takedown

If you consider content in White Rose Research Online to be in breach of UK law, please notify us by emailing eprints@whiterose.ac.uk including the URL of the record and the reason for the withdrawal request.

eprints@whiterose.ac.uk
https://eprints.whiterose.ac.uk/

Improved Temperature Performance of 1.31-μm Quantum Dot Lasers by Optimized Ridge Waveguide Design

S. K. Ray, K. M. Groom, R. A. Hogg, H. Y. Liu, M. Hopkinson, T. Badcock, D. J. Mowbray, and M. S. Skolnick

***Abstract*—In this letter, we demonstrate the importance of the fabricated device structure for the external differential efficiency, threshold current density, and maximum operating temperature for ground state operation of a 1.31-μm quantum dot laser. The introduction of a shallow ridge etch design and selective electroplating of the gold bondpads is demonstrated to offer improved performance in comparison to a deep ridge etch design with thinner evaporated gold bondpads.**

***Index Terms*—Dot-in-well (DWELL), quantum dots (QDs).**

I. Introduction

IDEAL quantum dot (QD) lasers are predicted to offer high gain, ultralow threshold current densities, and temperature-insensitive operation [1]. In order to realize these predictions, considerable emphasis has been placed on the optimization of structural parameters through a careful choice of the growth conditions. In addition, through the introduction of p-type delta doping of the QDs, recent reports have shown substantial improvements in the high-temperature performance [2], [3], a vital development if QD lasers are to be commercially viable. Within studies of QD laser characteristics, the specific fabrication parameters of the laser device are often not discussed. However, the optimization of these parameters are very important; for example, we have observed that the choice of ridge etch depth or the use of selectively electroplated gold bond pads can give significant improvements in device performance at high temperatures. In this letter the influence of the fabricated laser device structure on the temperature behavior of the operating characteristics of 1.3-μm QD lasers is reported.

II. Growth and Fabrication

The QD laser diode structures were grown in a solid-source VG Semicon V90H molecular beam epitaxy system on Si-doped GaAs (100) substrates. Each dot-in-well (DWELL) layer consisted of 3.0 monolayers of InAs grown on 2 nm of $In_{0.15}Ga_{0.85}As$ and covered by 6 nm of $In_{0.15}Ga_{0.85}As$. Five InAs–InGaAs DWELLs were separated by 50-nm GaAs barriers and embedded between 150-nm separate confinement heterostructure GaAs layers. Optical confinement was achieved using 1500-nm $Al_{0.4}Ga_{0.6}As$ cladding layers. The lower n-doped cladding layer was doped with Si at 5×10^{18} cm^{-3} while the upper p-cladding layer was doped with Be at 5×10^{17} cm^{-3}. The upper p-doped layer was completed by a 300-nm GaAs layer doped at 1×10^{19} cm^{-3}. Growth temperatures were 620 °C for the AlGaAs and 510 °C for the In containing layers. Following the deposition of each DWELL, the initial 15 nm of the GaAs spacer layer was deposited at 510 °C. Next, the temperature was increased to 580 °C for the remaining 35 nm. The temperature was then decreased back to 510 °C for the growth of the next DWELL. Areal dot densities of $\sim 4 \times 10^{10}$ cm^{-2} per layer were measured by atomic force microscopy on uncapped structures [4], [5]. The energy separation between ground and excited state transitions for this sample, as measured by PL spectroscopy, was ~50 meV.

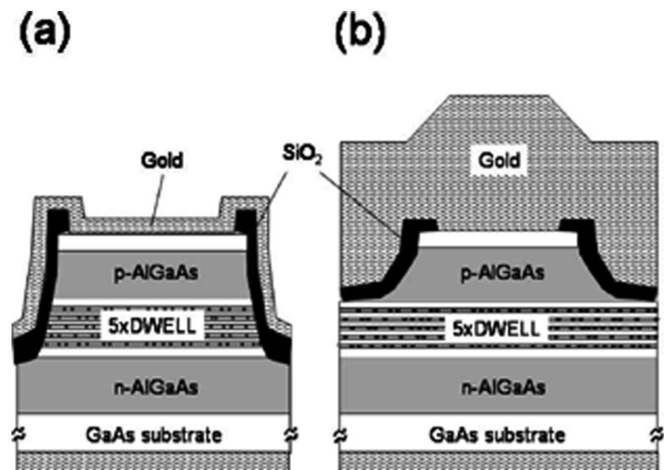

Fig. 1. (a) Schematic diagram of fully etched, and (b) shallow etched ridge waveguide with selective gold electroplating.

In the present study, two device designs were fabricated and characterized, these are shown schematically in Fig. 1(a) and (b). The devices are formed with either a deep ridge etch (Device A), or a shallow ridge etch (Device B). Device B also benefits from the incorporation of selectively electroplated gold bondpads. The deep etched device (Device A) is etched completely through the intrinsic region and into the lower n-doped AlGaAs

Manuscript received March 9, 2005; revised May 13, 2005. This work was supported by the U.K. EPSRC under Grant GR/S49308/01, and by the EC GROWTH Programme NANOMAT Project under Contract G5RD-CT-2001-00545.

S. K. Ray, K. M. Groom, R. A. Hogg, H. Y. Liu, and M. Hopkinson are with the EPSRC National Centre for III–V Technologies, Department of Electronic and Electrical Engineering, University of Sheffield, Sheffield S1 3JD, U.K. (e-mail: s.k.ray@shef.ac.uk; k.m.groom@shef.ac.uk; r.hogg@shef.ac.uk; h.liu@shef.ac.uk; m.hopkinson@shef.ac.uk).

T. Badcock, D. J. Mowbray, and M. S. Skolnick are with the Department of Physics and Astronomy, University of Sheffield, Sheffield S3 7RH, U.K. (e-mail: t.badcock@shef.ac.uk; d.mowbray@shef.ac.uk; m.skolnick@shef.ac.uk).

Digital Object Identifier 10.1109/LPT.2005.853530

1041-1135/$20.00 © 2005 IEEE

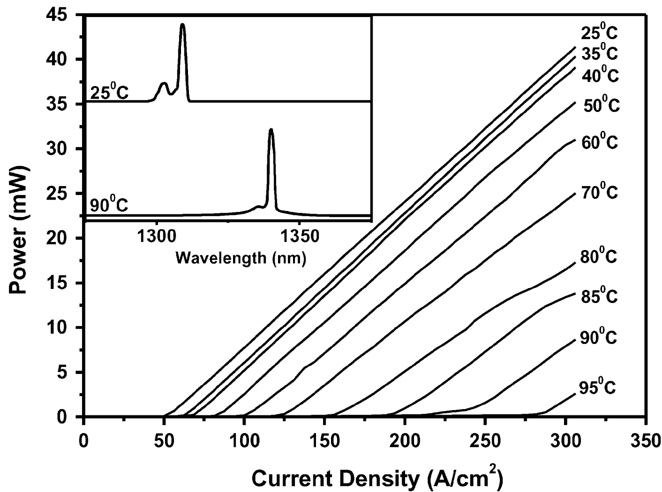

Fig. 2. Temperature-dependent L–I curves for a full-etched 4-mm-long cavity (Device A).

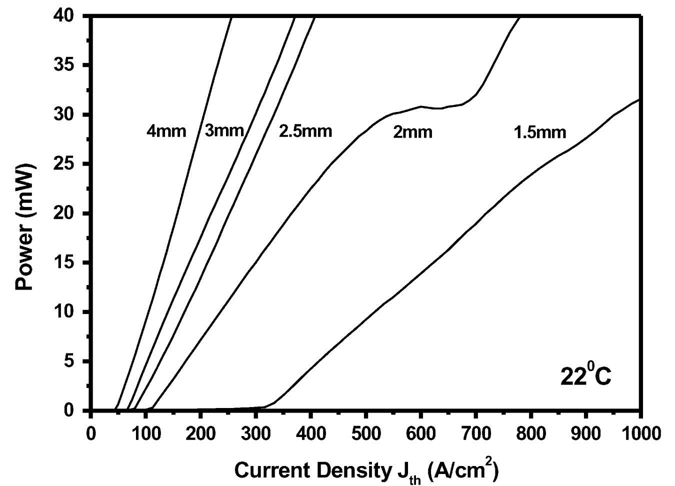

Fig. 3. L–I curves for full-etched devices of different cavity length (Device A).

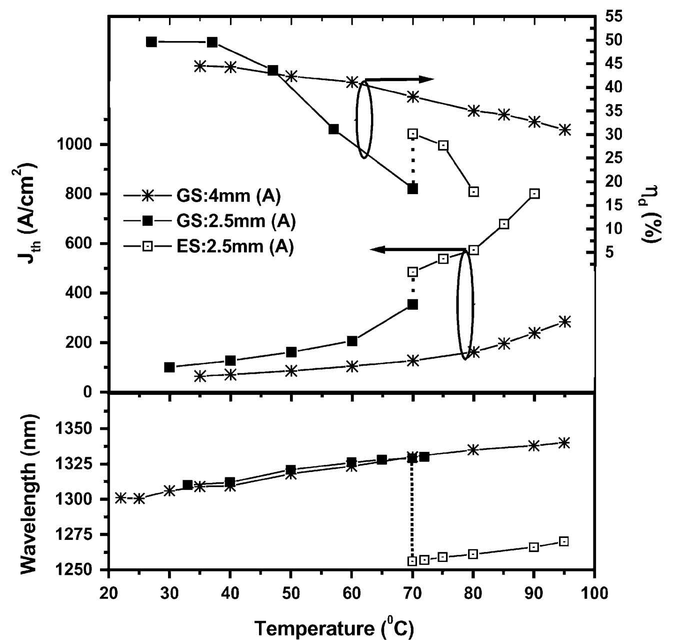

Fig. 4. Temperature dependence of threshold current density and the external quantum efficiency for 4 and 2.5 mm full-etched cavity.

region using $SiCl_4$-based reactive ion etching. The total depth of etching is 3.2 μm. The shallow etched devices were fabricated using a $SiCl_4$ based inductively coupled plasma technique with etching stopped once the p-doped AlGaAs layers were removed to a depth of 1.8 μm. This is achieved by *in situ* monitoring of the etch depth using a laser reflectometer. For both types of device, 500 nm of SiO_2 was deposited on the sample surface and contact windows opened on the ridge top. AuZnAu contact layers were deposited and annealed at 360 °C. The shallow etched devices were selectively electroplated with $\sim$3 μm of gold, compared to a typical evaporated gold thickness of $\sim$250 nm as applied to the deep etched devices. A range of ridge widths and cavity lengths were studied. However, all ridge widths demonstrated similar behavior and only results for a single ridge width (20 μm) are presented below.

III. Results and Discussion

Fig. 2 shows the current-power characteristics over a range of temperatures for a 4-mm cavity length, full ridge etch device (Device A). The inset shows lasing spectra at $1.1 \times J_{\rm th}$ at 25 °C and 90 °C. Lasing occurs via the ground state transition up to 120 °C. As the temperature is increased, the lasing wavelength increases gradually from a value of 1.31 μm at room temperature. Devices fabricated from the same wafer as the present devices have been shown previously to exhibit extremely low room temperature threshold and transparency current densities (transparency current density $\sim$1.5 A/cm^2/QD layer) [6]. Room temperature light output versus current curves (L–I), exhibited by Device Type A ridges of different cavity lengths, are shown in Fig. 3. A kink is observed in the L–I characteristic of the 2-mm-long device, which corresponds to a switching of the lasing wavelength. Longer devices lase via the ground state for all drive currents. In contrast, for a current density $\sim$600 A/cm^2, a 2-mm cavity [6], lases simultaneously at 1.31 and 1.23 μm, corresponding to the wavelengths of the QD ground and excited state transitions. For shorter cavity lengths, lasing is only observed from the excited state. The origin of the kink in the L–I characteristic of the 2-mm device is, therefore, attributed to a switching of the lasing wavelength from the ground state to the first excited state. This state switching occurs without hysterisis and is attributed to gain saturation of the QD ground state and incomplete gain clamping, leading to lasing from the excited state [7].

The temperature sensitivity of two fully etched (Device Type A) QD lasers of different cavity length is compared in Fig. 4, with threshold current density, external differential efficiency, and lasing wavelength plotted as a function of temperature. For the 4-mm-long device, only a relatively small change in both the threshold current density (characteristic temperature $T_0 = 53$ K from 20 °C to 70 °C) and the differential efficiency is observed up to 100 °C. In contrast, the 2.5-mm-long device exhibits a more pronounced reduction in differential efficiency together with a larger increase in threshold current density with temperature ($T_0 = 38$ K). In addition, for the 2.5-mm-long device, a discontinuity in both the threshold current density and

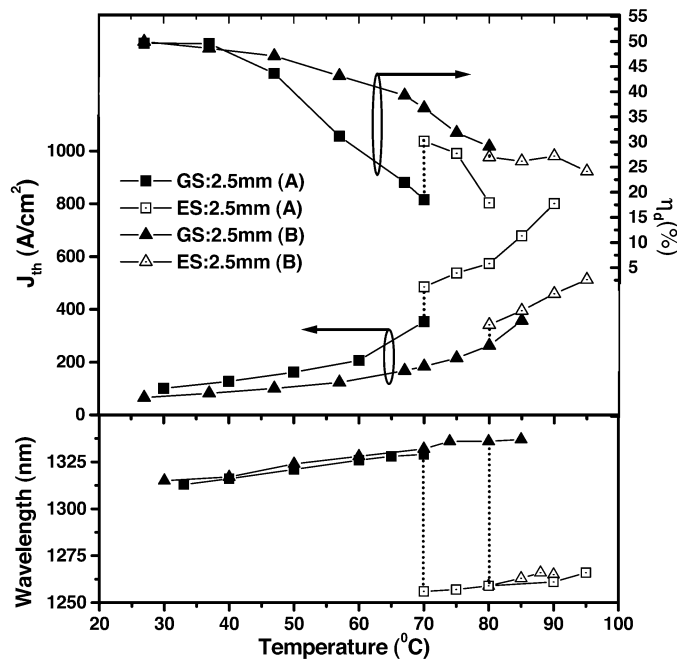

Fig. 5. Temperature dependence of threshold current density and external quantum efficiency for (A) deep etched device and (B) a shallow etched and electroplated device.

differential efficiency is observed at 70 °C, a result of lasing switching from the ground to the excited state. The value of the excited state threshold current density during the simultaneous lasing regime has been obtained by extrapolating the high current region of the characteristic back to the horizontal axis. The emission wavelength for the 2.5-mm-long device switches from 1.33 to 1.26 μm at 70 °C. The similar wavelengths and rate of change of wavelength with temperature in Fig. 4 indicate that the dominant process affecting the lasing wavelength is temperature, with carrier density effects making a smaller contribution.

The increased temperature sensitivity of the 2.5-mm-long cavity device is attributed to a comparatively higher excited state carrier population. The average dot carrier occupancy increases with decreasing cavity length, as a higher threshold gain is required. Even for ground state lasing, with the majority of carriers in the ground state, there will be a significantly higher occupation of the excited state in shorter cavity devices. This is due to a reduction in the carrier capture time of the ground state due to pauli blocking. As carriers in excited states are more likely to be lost from the dots by thermal excitation, an increased excited state carrier occupancy results in an increased device temperature sensitivity.

Fig. 5 compares the temperature behavior of the lasing wavelength, threshold current density, and external efficiency of two 2.5-mm cavity length devices, one shallow etched (Device B) and the other fully etched (Device A). Lasing for the fully etched device switches from the ground state at 70 °C, whereas the onset of this transition is delayed until 80 °C in the shallow etched device. The wavelength switching does not occur at a specific lasing wavelength (which would indicate a common cavity temperature) indicating that improved heat sinking is not the primary reason for the improved temperature performance of the shallow etched device. From Fig. 5, it is also evident that the shallow etched and selectively electroplated devices yield a lower $J_{\rm th}$ and higher differential efficiency at all temperatures, in comparison with the deep etched devices. Between 20 °C and 70 °C, the characteristic temperature T_0 is 38 K for Device Type A and 48 K for Device Type B.

The reasons for the improvement in temperature stability of the shallow etched and selectively electroplated devices are threefold; reduced optical loss from the etched ridge sidewall, reduced electrical loss from this etched semiconductor surface, and improved heat dissipation resulting from the thicker gold bond-pads. These combined effects are expected to result in the lasing threshold occurring at a lower carrier density, and hence lower average dot carrier occupancy, at all temperatures. As a result, there is a concomitant reduction of the excited state carrier occupancy, leading to an improved temperature stability.

In summary, the importance of the fabricated device design for the temperature stability of the threshold current density, onset of excited state lasing, and the external efficiency has been demonstrated for 1.3-μm QD lasers. An improvement in all three parameters is observed for devices with a shallow etched ridge structure and selectively electroplated gold bondpads, in comparison with a full ridge etched structure with thin evaporated gold bondpads.

Acknowledgment

The authors gratefully acknowledge useful discussions with D. Robbins and D. Childs of Bookham Technologies.

References

[1] Y. Arakawa and H. Sakaki, "Multidimentional quantum well laser and temperature dependence of its threshold current," *Appl. Phys. Lett.*, vol. 40, pp. 939–941, Jun. 1982.

[2] S. Fathpour, Z. Mi, P. Bhattacharya, A. R. Kovsh, S. S. Mikhrin, I. L. Krestnikov, and N. N. Ledentsov, "The role of Auger recombination in the temperature-dependent output characteristics ($T_0 = \infty$) of p-doped 1.3 μm quantum dot lasers," *Appl. Phys. Lett.*, vol. 85, pp. 5164–5166, 2004.

[3] K. Otsubo, N. Hatori, M. Ishida, S. Okumura, T. Akiyama, Y. Nakata, H. Ebe, M. Sugawara, and Y. Arakawa, "Temperature-insensitive eye-operating under 10-Gb/s modulation of 1.3 μm P-doped quantum-dot lasers without current adjustment," *Jpn. J. Appl. Phys.*, vol. 43, no. 8B, pp. L1124–L1126, 2004.

[4] H. Y. Liu, I. R. Sellers, T. J. Badcock, D. J. Mowbray, M. S. Skolnick, K. M. Groom, M. Gutierrez, M. Hopkinson, J. S. Ng, J. P. R. David, and R. Beanland, "Improved performance of 1.3 μm multiplayer InAS/GaAs quantum dot laser using a high-growth-temperature GaAs spacer layer," *Appl. Phys. Lett.*, vol. 85, pp. 704–706, 2004.

[5] H. Y. Liu, I. R. Sellers, M. Gutierrez, K. M. Groom, W. M. Soong, M. Hopkinson, J. P. R. David, R. Beanland, T. J. Badcock, D. J. Mowbray, and M. S. Skolnick, "Influence of the spacer layer growth temperature on multiplayer InAs/GaAs quantum dot structure," *J. Appl. Phys.*, vol. 96, pp. 1988–1992, 2004.

[6] S. K. Ray, K. M. Groom, H. Y. Liu, M. Hopkinson, R. A. Hogg, I. R. Seller, T. Badcock, A. J. Ramsay, D. J. Mowbray, and M. S. Skolnick, "Growth, fabrication and operating characteristics of ultra-low threshold 1.31 μm quantum dot lasers," *Jpn. J. Appl. Phys.*, vol. 44, no. 4B, pp. 2520–2522, 2005, to be published.

[7] A. Markus, J. X. Chen, C. Paranthoen, C. Platz, O. Gauthier-Lafaye, and A. Fiore, "Simultaneous two-state lasing in quantum dot lasers," *Appl. Phys. Lett.*, vol. 82, pp. 1818–1820, 2003.